Stem Cells Translational Medicine, 2025, **14**, szaf064
https://doi.org/10.1093/stcltm/szaf064
Original Research

Harnessing 3D cultured MSC exosomes through tangential flow filtration for enhanced diabetic wound healing

Yanmei Chen[1,#], Yang Xu[2,3,#], Yali Zheng[1,#], Yingda Yan[1], Jiawei Cai[1], Chu Hua[1], Jiang Li[1], Cheng Zhang[1,4], Marianne Lauwers[2,3,5], Ying Rao[2,3], Zhenyu Zhong[2,3,5], Dai Fei Elmer Ker[6], Rocky S. Tuan[2,3,5,7], Xiao Yang[8,9,*], Dan Michelle Wang[2,3,5,7,*], Zhiyong Zhang[1,*]

[1]Translational Research Centre of Regenerative Medicine and 3D Printing, Department of Orthopaedic Surgery, Guangzhou Key Laboratory of Spine Disease Prevention and Treatment, Guangdong Province Engineering Research Center for Biomedical Engineering, State Key Laboratory of Respiratory Disease, Guangdong Provincial Key Laboratory of Major Obstetric Diseases, Guangdong Provincial Clinical Research Center for Obstetrics and Gynecology, The Third Affiliated Hospital, Guangzhou Medical University, Guangzhou, Guangdong, China
[2]School of Biomedical Sciences, Faculty of Medicine, The Chinese University of Hong Kong, Hong Kong SAR, China
[3]Institute for Tissue Engineering and Regenerative Medicine, The Chinese University of Hong Kong, Hong Kong SAR, China
[4]REGEN-αGEEK Biotechnology Co.Ltd, Haining, China
[5]Center for Neuromusculoskeletal Restorative Medicine, Hong Kong Science Park, Shatin, New Territories, Hong Kong SAR, China
[6]Department of Biomedical Engineering, The Hong Kong Polytechnic University, Hong Kong SAR, China
[7]Department of Orthopaedics and Traumatology, Faculty of Medicine, The Chinese University of Hong Kong, Hong Kong SAR, China
[8]Department of Ultrasound, Peking Union Medical College Hospital, Chinese Academy of Medical Sciences and Peking Union Medical College, Beijing, China
[9]Zhangzhou Municipal Hospital Affiliated to Fujian Medical University, Zhangzhou, Fujian, China

[*]Corresponding authors. Xiao Yang, Department of Ultrasound, Peking Union Medical College Hospital, Chinese Academy of Medical Sciences and Peking Union Medical College, Beijing, China; Zhangzhou Municipal Hospital Affiliated to Fujian Medical University, Zhangzhou, Fujian, China. E-mail: yangxiao1@pumch.cn; Dan Michelle Wang, School of Biomedical Sciences, Faculty of Medicine, The Chinese University of Hong Kong, Hong Kong SAR, China; Institute for Tissue Engineering and Regenerative Medicine, The Chinese University of Hong Kong, Hong Kong SAR, China; Center for Neuromusculoskeletal Restorative Medicine, Hong Kong Science Park, Shatin, New Territories, Hong Kong SAR, China; Department of Orthopaedics and Traumatology, Faculty of Medicine, The Chinese University of Hong Kong, Hong Kong SAR, China. E-mail: wangmd@cuhk.edu.hk; Zhiyong Zhang, Translational Research Centre of Regenerative Medicine and 3D Printing, Department of Orthopaedic Surgery, Guangzhou Key Laboratory of Spine Disease Prevention and Treatment, Guangdong Province Engineering Research Center for Biomedical Engineering, State Key Laboratory of Respiratory Disease, Guangdong Provincial Key Laboratory of Major Obstetric Diseases, Guangdong Provincial Clinical Research Center for Obstetrics and Gynecology, The Third Affiliated Hospital, Guangzhou Medical University, Guangzhou, Guangdong, China. E-mail: drzhiyong_pa@126.com.
[#]These authors contributed equally to this work.

Abstract

Introduction: Mesenchymal stem cell-derived exosomes have garnered considerable attention in regenerative medicine due to their non-immunogenicity, low infusion toxicity, easy accessibility, straightforward preservation, and minimal ethical concerns. While ultracentrifugation is the prevailing method for high-purity exosome isolation, it is limited by low throughput and the need for specialized infrastructure. This study investigates tangential flow filtration (TFF) as a promising alternative for exosome isolation. This technique offers simpler operation, higher yields, and improved recovery rates compared to ultracentrifugation.

Methods: Human umbilical cord mesenchymal stem cells (hUCMSCs) were cultured in a 3D microcarrier-bioreactor system, and exosomes were extracted from the conditioned medium using either ultracentrifugation or an automated and enclosed TFF system. Subsequently, we compared the quantity, quality and therapeutic efficacy of the exosomes isolated via both approaches, evaluating their effects *in vitro* and in a mouse model of diabetic wound healing.

Results: Our findings demonstrate that the TFF method effectively isolates high-quality exosomes that meet the standards set by the Minimum Information for Studies of Extracellular Vesicles (MISEV) 2023 guidelines, while achieving a significantly higher extraction yield compared to the traditional ultracentrifugation. Furthermore, both TFF and ultracentrifugation-derived exosomes demonstrate comparable biological activity *in vitro* and similar therapeutic potential for treating diabetic wound healing, potentially through promoting M2 macrophage polarization and angiogenesis.

Conclusion: The results indicate that TFF is a viable method for scalable and efficient exosome production, facilitating advancements in clinical applications for diabetic wound repair.

Key words: exosomes, stem cells, tangential flow filtration, ultracentrifugation, diabetic wound healing.

Received: 2 June 2025; **Accepted:** 13 October 2025.

Graphical abstract

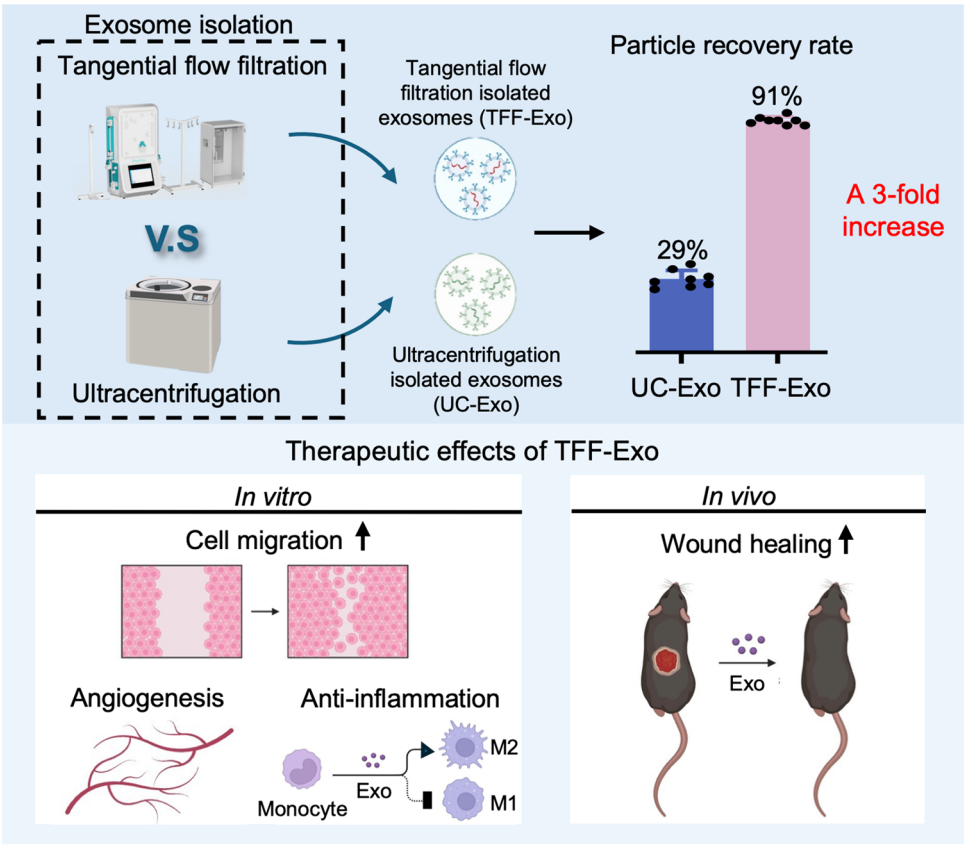

Significance Statement

Tangential flow filtration (TFF) offers an exosome isolation method with simpler operation that can achieve higher yields and increased recovery rates of isolated exosomes compared to ultracentrifugation. In our study, the high-quality exosomes produced with TFF meet safety standards and demonstrate comparable functionality to ultracentrifugation-derived exosomes in both in vivo and in vitro models. Moreover, the TFF method achieving an almost complete recovery rate (91%) compared to the traditional ultracentrifugation method (29%). These results further laid the foundation for the application of TFF and TFF-derived exosomes in the regeneration medicine.

1. Introduction

Mesenchymal stem cell (MSC)-derived exosomes are lipid bilayer vesicles ranging from 20 to 200 nm in diameter. These vesicles encapsulate proteins, lipids, biofactors, and genetic materials, and present valuable potential in regenerative medicine applications.[1] Therapeutic potential spans various conditions, such as cardiovascular diseases, diabetes, osteoarthritis, and wound healing.[2–9] Despite their promise, significant variability in extraction methods complicates the standardization of manufacturing procedures and limits large-scale production. This inconsistency poses challenges for the clinical translation of exosomes.[10–13] Traditional techniques for isolating exosomes from cell culture medium include ultracentrifugation, ultrafiltration, size exclusion chromatography, polymer precipitation, and density gradients.[12] Among these, ultracentrifugation has long been the standard method for exosome isolation.[14] However, ultracentrifugation is associated with low yields, high time demands, and labor-intensive repeated centrifugation steps.[15]

To address these limitations, tangential flow filtration (TFF) has emerged as a rapid and efficient method for isolating and purifying exosomes from large volumes of cell culture medium.[16] TFF devices utilize size-based sieving with nanoporous membranes to effectively separate exosomes from other components in the medium. The tangential flow design mitigated common challenges associated with vertical filtration methods, such as high pressure and clogging.[17] Additionally, TFF devices are relatively easy to fabricate, with low operational and fabrication costs. Importantly, TFF offers high exosome separation efficiency, yielding favorable results within a short timeframe.[16] While ultracentrifugation processing can take approximately 14 hours, TFF can achieve comparable outcomes in under three hours.[17] Moreover, TFF can handle a wide range of sample volumes, from 10 mL to several thousand liters.[17] Overall, the adoption of TFF has significant potential to enhance the efficiency and reliability of exosome extraction, and advance both exosome research and therapeutic applications.[18]

While studies have shown that TFF significantly enhances exosome yield, purity, and processing time compared to conventional ultracentrifugation methods,[19] there are still some limitations associated with TFF-based exosome extraction. One key issue is that many steps in both ultracentrifugation and TFF manufacturing processes involve open systems, which increase the risk of contamination and product loss. Additionally, conventional sterilization methods, such as terminal sterilization, are often incompatible with exosome products, further elevating the risk of contamination.[20] To mitigate these risks, it is preferable to conduct the entire manufacturing process within a closed system.[20] However, closed systems may offer less flexibility for future procedural modifications. Therefore, developing a tunable and enclosed TFF system could provide significant operative advantages. Furthermore, transitioning from manual to automated processes, equipped with real-time monitoring and measurements, will be crucial in enhancing the overall efficiency and reliability of exosome production.

To address these challenges, our laboratory has developed a tunable, automated, enclosed TFF system (DASEA® ReGenbio, China) specifically for stem cell exosome extraction. This system integrates multi-stage filtration with tangential flow technology, enabling efficient, rapid, and scalable exosome recovery.[18] Key features of the system include a closed design, comprehensive parameter monitoring (including transmembrane pressure (TMP), weight, concentration and replacement factors), performance testing for water flux and membrane integrity, low-temperature protection to maintain the integrity and biological activity of exosomes during collection.[18] Additionally, the automated processing simplifies operation, while its flexible configuration allows adaptation to various process and buffer system requirements.

Beyond the design of TFF exosome extraction systems, further characterization of the quality and therapeutic efficacy of the exosomes is critical for clinical applications. Application of exosomes as a cell-free approach has been widely studied in the enhancement of diabetic wound healing.[21] Diabetic wounds represent a complex clinical condition characterized by poor closure, scarring, infection, and delayed healing, significantly impacting patients' quality of life and presents a significant burden on the healthcare system.[22,23] Our previous study on the automated and enclosed three-dimensional (3D) biofabrication system for culturing human umbilical cord mesenchymal stem cells (hUCMSCs) highlights the enhanced biological characteristics and therapeutic potential of these cells for diabetic wound healing.[24] The study underscores the limitations of traditional two-dimensional (2D) culture systems, demonstrating that 3D culture significantly improves cell yield, migration, angiogenesis, and anti-inflammatory responses.[24] In contrast, in the current study, we aim to investigate the efficacy of exosomes generated from hUCMSCs in the same 3D biofabrication system and collected through advanced TFF methods in promoting wound healing. Therefore, we initially cultured human umbilical cord mesenchymal stem cells (hUCMSCs) using bionic microcarriers® and a bioreactor system to enhance the isolation of bioactive exosomes, achieving higher yields compared to traditional two-dimensional (2D) culture methods.[25,26] We next characterized the morphology, particle size and surface markers of the exosomes extracted via ultracentrifugation and our automated and enclosed TFF system using transmission electron microscopy (TEM), Western blot (WB), and nanoparticle tracking analysis (NTA). Furthermore, we assessed the uptake of exosomes by cells and effects of these exosomes on cell viability, migration, as well as their pro-angiogenic and anti-inflammatory properties. We also evaluated their potential mechanisms of their bioactive efficacy, with a particular focus on angiogenesis and anti-inflammatory effects, in a mouse diabetic wound healing model (Figure 1A).

2. Materials and methods

2.1. 3D culture of hUCMSCs

Human umbilical cord tissue was obtained from four different healthy donors in accordance with the guidelines set by the Institutional Ethics Review Board of the Third Affiliated Hospital of Guangzhou Medical University (Permit Number: 2020_001). hUCMSCs were isolated and cultured as previously described.[24] Briefly, fresh human umbilical cords were collected, cut into small pieces (1 to 8 cm^3) and cultured in serum-free hMSC culture UltraMedia (RGM0051, REGEN-αGEEK Biotechnology CO., LTD, China) in a humidified incubator with 5% CO_2 at 37 °C.[24] The cells isolated from the umbilical cord tissue were characterized with flow cytometry, trilineage differentiation assay, soft agar colony formation assay, cell chromosome analysis, and short tandem repeat analysis as described in our previous study.[24]

For the 3D culture of hUCMSCs, 6×10^7 hUCMSCs at passage 3 were mixed with 3 g of 3D bionic microcarriers® (RC001LE, REGEN-αGEEK Biotechnology CO., LTD, Haining, China) in 700 mL of serum-free hMSC culture UltraMedia. This mixture was inoculated into a sterile 2 L benchtop bioreactor (3D aBioR-02-CC, REGEN-αGEEK Biotechnology CO., LTD, Haining, China). An additional volume of serum-free culture medium was added 24 hours after inoculation to reach a total volume of 2 L. The cells were cultured for a duration of 5-7 days.

2.2. Extraction of exosomes from 3D cultured-hUCMSCs

The conditioned culture medium from the 5-day cultured 3D-hUCMSCs of 4 different donors was collected separately and cells from every donor divided into two equal portions for exosome extraction, using either ultracentrifugation or the TFF method. For ultracentrifugation extraction, the culture medium was subjected to differential centrifugation at 4 °C as previously reported,[27] namely initial centrifugation at 300 × g for 10 minutes, then at 2000 × g for 20 minutes, and finally at 10,000 × g for 30 minutes. This procedure removed any remaining cells and cell debris from the culture medium. The medium was then filtered through a 0.22 μm filter (polyethersulfone, PES, membrane) to remove microorganisms and large vesicles. Finally, the supernatant was subjected to ultracenfugation at 100,000 × g for 90 minutes using a Beckman Coulter Optima XPN-80 ultracentrifuge. The exosome pellet was resuspended in physiological saline, labelled as ultracentrifugation-Exo and stored at −80°C until use.

For the TFF extraction method, the hUCMSC culture supernatant was subjected to the DASEA ReGenbio automated exosome collection system (aColl-10-EXO, REGEN-αGEEK Biotechnology CO., LTD, Haining, China). Briefly, the supernatant from 3D-hUCMSCs was first filtered through a 1 μm filtration membrane (PES membrane) to eliminate detached

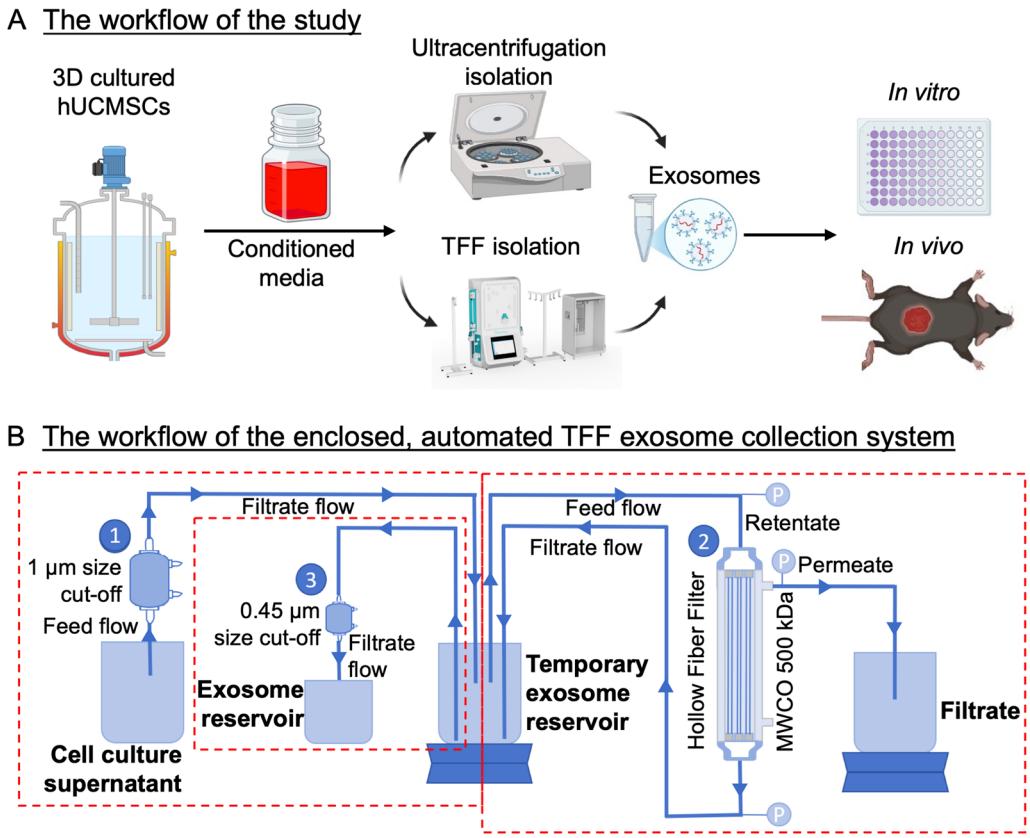

Figure 1. Study schematics. (A) The study workflow: conditioned media preparation, exosome isolation, and *in vitro*/*vivo* characterizations of exosomes. (B) A schematic illustration of an enclosed, automated tangential flow filtration (TFF) exosome collection system. In the first compartment, the supernatant derived from 3D-hUCMSCs is filtered through a 1 μm filtration membrane to eliminate detached cells, large debris, and larger particles. Subsequently, a hollow fiber filter with a molecular weight cut-off (MWCO) of 500 kDa is employed in the TFF system for the ultrafiltration of the supernatant. Finally, the product is subjected to sterile filtration using a 0.45 μm filter in the third part to obtain a physiological saline filtrate containing exosomes.

cells, large debris, and larger particles. Subsequently, a hollow fiber filter (modified PES (mPES), fiber diameter 0.5 mm, filtration area 0.15 cm^2/m^2, 320 fibers) with a molecular weight cutoff (MWCO) of 500 kDa was employed in the TFF system for ultrafiltration of the supernatant. Throughout the filtration process, the feed flow rate (PFeed) was maintained at 120 mL/min, and TMP was maintained at less than 3.5 psi. The supernatant was concentrated tenfold (volume reduced by a factor of ten), followed by buffer recirculation and dialysis. During dialysis, the existing buffer was replaced with an equal volume of physiological saline, with a small amount of physiological saline recirculated through the system for 10 minutes to ensure efficient buffer exchange. Finally, the product was subjected to sterile filtration using a 0.45 μm PES filter to obtain a physiological saline containing exosomes. Prior to processing the exosome products, the 0.45 μm filter was washed with sterile phosphate-buffered saline (PBS) (pH 7.4) and 20% ethanol, followed by a rinse with sterile PBS. For post-processing, the membrane was cleaned with sterile PBS and 0.5 M NaOH and then stored at 4 °C (Figure 1B). The exosomes derived from the TFF method were labelled as TFF-Exo and stored at −80°C until use.

2.3. Characterization of ultracentrifugation-Exo and TFF-Exo

Ultracentrifugation-Exo and TFF-Exo were characterized as follows. (1) The exosome recovery rate was calculated as follows: Exosome recovery rate (%) = [particle yield in exosome reservoir)/(particle yield in cell culture supernatant)] × 100%. (2) For TEM analysis, 20 μL of the exosome suspension was pipetted onto a copper grid and dried under an infrared lamp for 10 minutes. Two drops of 2% phosphotungstic acid solution were added for negative staining, followed by another 10-minute drying under the infrared lamp. Exosome morphology was imaged using TEM. (3) For WB analysis, total protein content was extracted from the exosome preparations isolated from cells from different donors. The proteins were fractionated by SDS-PAGE. WB analysis was performed using following antibodies calnexin (1:2000; 2679S, CST), TSG101 (ET1701-59, HUABIO, China), CD9 (1:2000; ab92726, Abcam), CD63 (1:1000; AF1471, Beyotime, China), and CD81 (1:1000; AG1530, Beyotime, China). (4) For NTA analysis, the exosomes isolated from different donors were resuspended in 1 mL of sterile water at a 1:1000 ratio. Particle concentration and size distribution were analyzed using a ZetaView NTA instrument (ZetaView, Particle Metrix, Germany).[28]

2.4. Detection of exosome uptake by cells

To assess the uptake of exosomes by National Institutes of Health 3T3 cells (NIH-3T3) (Pricella, China), human umbilical vein endothelial cells (HUVECs) (Pricella, China), and M0 macrophages (Raw 264.7 cells) (Pricella, China), we labelled TFF-Exo and ultracentrifugation-Exo with red fluorescent PKH26 (Sigma-Aldrich, USA) according to the manufacturer's

instructions. Briefly, a working solution of 1 μM PKH26 dye was added to the exosomes (10^11 particles/mL) and incubated in the dark at room temperature for 10 minutes. Following this, an equal volume of Exosome-free Fetal Bovine Serum (Umibio, Shanghai, China) was added to quench any unbound dye. The labelled exosomes were then centrifuged at 100,000 × g for 120 minutes at 4 °C to remove excess dye, and the exosomes were resuspended in 200 μL of PBS.

NIH-3T3, HUVECs, and Raw 264.7 cells were previously seeded in glass bottom cell culture dishes (NEST Biotechnology) to achieve 70-80% confluence prior to co-culture. The PKH26-labelled exosomes or an equal volume of control PKH26-PBS were then added to the cells and incubated for 24 hours. After incubation, the cells were washed with PBS, fixed with 4% paraformaldehyde for 20 minutes, and permeabilized with 0.1% Triton X-100 for 10 minutes. Finally, the cells were incubated with Phalloidin-IF488 (Servicebio, Wuhan, China) for 60 minutes to stain F-actin and DAPI (Invitrogen, USA) to stain the nuclei. The uptake of PKH26-labelled exosomes by the cells was subsequently observed using a microscope (OLYMPUS IX83, Japan).

2.5. Cytocompatibility of ultracentrifugation-Exo and TFF-Exo

To assess the cytocompatibility of ultracentrifugation-Exo and TFF-Exo, the cell viability of HUVECs and NIH-3T3 was evaluated after a 24-hour culture in exosome-containing medium, using Cell Counting Kit-8 (CCK8, Beyotime, C0037, China) assay and Calcein AM/Propidium Iodide (PI) staining.

In the CCK8 assay, HUVECs and NIH-3T3 were separately seeded onto 96-well plates at a density of 3,000 cells/well and cultured for 24 h to ensure full adherence. The cells were then treated with isolated exosomes (either the TFF-Exo or ultracentrifugation-Exo) at a concentration of 10,000 particles per cell with an untreated group serving as control. After 24 hours of co-culture, the culture medium was replaced with medium containing 10% CCK-8 reagent (GLPBIO, USA). The cells were incubated for additional 2 hours at 37 °C, and the absorbance at 450 nm was measured using a microplate reader (Tecan M200 pro, Switzerland). The cell viability of the TFF-Exo group and ultracentrifugation-Exo group was calculated using the following formula: Cell viability (%) = [1 – (A_{450} treated—A_{450} blank)/(A_{450} control—A_{450} blank)] × 100%.

For Calcein AM/PI staining, HUVECs and NIH-3T3 were separately seeded onto 96-well plates at a density of 3,000 cells/well and cultured for 24 hours to ensure full adherence. Subsequently, the cells were treated with exosomes (10,000 particles per cell) for 48 hours, the cells were stained according to the instructions of the Calcein/PI cell viability and cytotoxicity detection kit (C2015M, Beyotime, China). Specifically, the cells were incubated with the staining solution at 37 °C in the dark for 30 minutes. The staining solution was then removed, and the cells were washed 2-3 times with PBS. Finally, 100 μL of PBS was added, and the cells were observed under a fluorescence microscope (OLYMPUS IX83, Japan). Cells emitting green fluorescence (calcein labelled) were considered viable, while cells emitting red fluorescence (ethidium bromide labelled) were identified as dead cells.

2.6. Cell migration assay

The migratory motility of HUVECs in response to different exosome treatments was assessed using the scratch assay and Transwell migration assay. In the scratch assay, HUVECs (3×10^5 cells/well) were seeded onto a 6-well plate and cultured until they reached over 95% confluence. A uniform cell-free area was created by scratching the cell monolayer using a 200 μL pipette tip. The area was washed three times with PBS to remove cellular debris, and the baseline was recorded under a microscope. The cells were then treated with either ultracentrifugation-Exo or TFF-Exo (10,000 particles per cell) and cultured for 24 hours. The untreated cell culture group served as the control group. The same scratch area was imaged again after 24 h. The cell migration rate was quantified with ImageJ software: Migration rate (%) = (scratch area at 24 h post-operation—scratch area at 0 h post-operation)/scratch area at 0 h post-operation × 100%.

In the Transwell migration assay, HUVECs were resuspended in serum-free culture medium at a concentration of 1×10^5 cells/mL. A 200 μL aliquot was seeded into the upper chamber of a transwell insert (8 μm pore size, Corning, USA). In the lower chamber, 800 μL of the culture medium containing 10% FBS was added. The experimental groups were treated with either TFF-Exo or ultracentrifugation-Exo at a dose of 10,000 particles per cell. The control group received no treatment. The Transwell inserts were then placed into the 24-well plate and cultured in a cell culture incubator at 37 °C for 24 hours. After incubation, the Transwell inserts were removed, and the cells on the upper surface of the membrane were gently washed off with PBS. Migrated cells on the bottom side were fixed with 4% paraformaldehyde, stained with crystal violet, and observed under a microscope (OLYMPUS IX83, Japan) to assess migration.

2.7. Endothelial tube formation assay

In the tube formation assay, HUVECs were used to investigate endothelial tube formation in response to different exosome treatments, as previously reported.[29] Specifically, HUVECs were pre-treated for 24 hours with either TFF-Exo or ultracentrifugation-Exo at a dosage of 10,000 particles per cell, while untreated HUVECs served as the control. The cells were then seeded into a 96-well plate pre-coated with Matrigel (Corning, USA) at a density of 5×10^3 cells per well. The cells were incubated at 37 °C with 5% CO_2. After 8 hours of culture, the tube-like structures formed were observed and imaged using a microscope. The images were analyzed using ImageJ software to quantify the number of branch points, junctions, and the total tube length in randomly selected fields of view for further statistical analysis.

2.8. Flow cytometry analysis

To test the anti-inflammatory effect of exosomes, flow cytometry was conducted. M0 macrophages were seeded into a 6-well plate at a density of 3×10^5 cells per well. After 24 hours of culture, cells were treated with LPS (100 ng/mL) for 24 hours to induce macrophage M1 polarization. The culture medium was then replaced with fresh medium containing either TFF-Exo or ultracentrifugation-Exo at a dose of 10,000 particles per cell in the experimental groups. The control group consisted of cells cultured in medium alone. After 24 hours of co-culture, the macrophages were collected by trypsinization and fixed/permeabilized using a flow cytometry fixation/permeabilization buffer (Invitrogen, USA) for 20 minutes. The cells were then stained with the following antibodies: FITC-conjugated anti-mouse CD206 antibody (1:150, BioLegend, USA) to detect M2

macrophages, and PE-conjugated anti-mouse CD86 antibody (1:150, BioLegend, USA) to detect M1 macrophages. The cells were incubated with the antibodies at 4 °C for 1 hour. Finally, the stained cells were analyzed using a flow cytometer (Attune NxT, Thermo Fisher), and the percentages of M1 and M2 macrophages were determined using the FlowJo 10.0 software.

2.9. In vivo diabetic wound model

To evaluate the *in vivo* pro-regenerative ability of the exosome, a 10 mm diameter, full thickness skin wound model was created in diabetic male C57BL/6J mice (Animal ethics number: G2024-1255). Specifically, healthy mice (male, 6 weeks, 20–25 g) were obtained from the Guangdong Provincial Medical Laboratory Animal Center. The mice were injected with streptozotocin (STZ, 125 mg/kg, Sigma-Aldrich, St Louis, MO, USA) in citrate buffer (pH 4.5) on day 1 to establish a diabetic model, as previously described.[30] Mice with persistent blood glucose levels above 16 mmol/L, measured in the tail vein, 7 days after the initial STZ injection were considered as a successful hyperglycemic model.

After successfully establishing the diabetic model, the mice underwent skin wound surgery. The mice were anesthetized with 1% sodium pentobarbital (50 mg/kg, i.p.). A full-thickness skin wound with a diameter of 10 mm was created on the dorsal side of the abdomen using surgical scissors.[31] Following the wound surgery, the 36 mice were randomly divided into three groups (n = 12 per group): (1) Control group: 0.1 mL physiological saline injected around the wound; (2) TFF-Exo treatment group: 0.1 mL physiological saline containing 1×10^{10} particles of TFF-Exo injected around the wound; (3) Ultracentrifugation-Exo treatment group: 0.1 mL physiological saline containing 1×10^{10} particles of ultracentrifugation-Exo injected around the wound. The process of wound closure was monitored by taking photographs of the wounds on days 0, 3, 6, and 9 post-surgeries. The wound closure rate was calculated based on images analyzed using ImageJ software as: (Initial wound area—Wound area on day n)/Initial wound area × 100%.

2.10. Exosome tracking assay in vivo

To conduct *in vivo* exosome tracking, TFF-Exo and ultracentrifugation-Exo were labelled with the lipophilic red fluorescent dye 1,1'-dioctadecyltetramethylindotricarbocyanine Iodide (DiR) (abs45153692, Absin, Shanghai, China) according to the manufacturer's instructions. Briefly, TFF-Exo and ultracentrifugation-Exo (10^11 particles/mL) were labelled with 2 μM DiR at 37 °C for 30 minutes. The labelled exosomes were then centrifuged at 100,000 × g for 120 minutes at 4 °C to remove excess dye, and the exosomes were resuspended in 1 mL of physiological saline. After modeling as outlined above, DiR-labelled exosomes (10^10 particles in 100 μL) were immediately injected into the surrounding area of the injured skin in mice. Bioluminescence imaging was performed at 3-, 12-, and 24-hours post-injection (*in vivo* imaging system, Tanon, ABL-X5, China).

2.11. Histology, immunohistochemistry, and RT-qPCR analysis

To evaluate the healing of diabetic wounds, histological analysis, immunohistochemical (IHC) staining and quantitative real-time PCR (RT-qPCR) were conducted. At day 9 post-surgery, all mice were euthanized by cervical dislocation. Skin tissue samples were harvested and fixed in 4% paraformaldehyde for 24 hours at room temperature. After fixation, the samples were embedded in paraffin. The paraffin-embedded skin samples were microtome-sectioned at 5 μm thickness (Automatic Microtome HM355S, Epredia, USA).

Histological evaluation, including hematoxylin and eosin (H&E) and masson's trichrome staining, were used to investigate the diabetic wound healing. All images of stained tissue slices were acquired using an optical microscope (Ni-U Eclipse Upright Microscope, Nikon, Japan). For IHC and immunofluorescence (IF) staining, the paraffin-embedded tissue sections were first deparaffinized, followed by antigen retrieval by heating the sections at 98 °C for 20 minutes in a citrate buffer (pH 6.0). After washing 3 times with PBS, the tissue sections were blocked with 5% bovine serum albumin for 30 minutes. The samples were then incubated overnight at 4 °C with the respective primary antibodies (CD31, α-SMA, CD86 and CD206, BioLegend, USA), washed, followed by incubation with appropriate horseradish peroxidase (HRP)- or fluorescein-labelled secondary antibodies. Following another 3 times wash with PBS, the HRP-antibodies treated sections were incubated with either 3, 3'-diaminobenzidine (DAB). Bright and fluorescent images were acquired using an inverted fluorescence microscope. The positive staining proportion in each field of view was quantified with ImageJ.

For RT-qPCR analysis, total RNA was extracted from each skin sample according to the manufacturer's instructions using a TRIzol-based RNA extraction kit (CWBIO, Jiangsu, China). 1 μg of the extracted RNA was reverse transcribed into complementary DNA (cDNA) using the Evo M-MLV Reverse Transcription Premixed Kit Ver.2 (Accurate Biotechnology CO., LTD, Changsha, China). RT-qPCR was performed using the SYBR Green qPCR kit (AG11718, Accurate Biotechnology CO., LTD, Changsha, China) on a QuantStudio 3 Real-Time PCR System (Thermo Fisher, USA). The following target genes were measured: (1) angiogenesis: platelet-derived growth factor (PDGF) and hypoxia-inducible factor-1α (HIF-1α); (2) fibroblast activation: collagen type I (Collagen I); (3) inflammatory response: iNOS, TNF-α, IL-1β, CD163, CD206, and TGF-β. GAPDH was used as the reference gene. Relative gene expression was quantified using the 2^(-ΔΔCt) method. The primer sequences used in this study are provided in Supplementary information, Table S1.

2.12. Statistical analysis

The data were analyzed, and graphical representations were generated using GraphPad Prism 7.0 software. All data are presented as mean ± standard error of the mean (SEM). For comparisons between multiple groups, one-way analysis of variance (One-way ANOVA) was performed, followed by Tukey's post-hoc test for pairwise comparisons. For comparisons between two groups, Student's t-test was used, with a significance level set at $p \leq 0.05$.

3. Results

3.1. Characterization of ultracentrifugation-Exo and TFF-Exo

The ultracentrifugation-Exo and TFF-Exo preparations were characterized in terms of morphology, size distribution, and

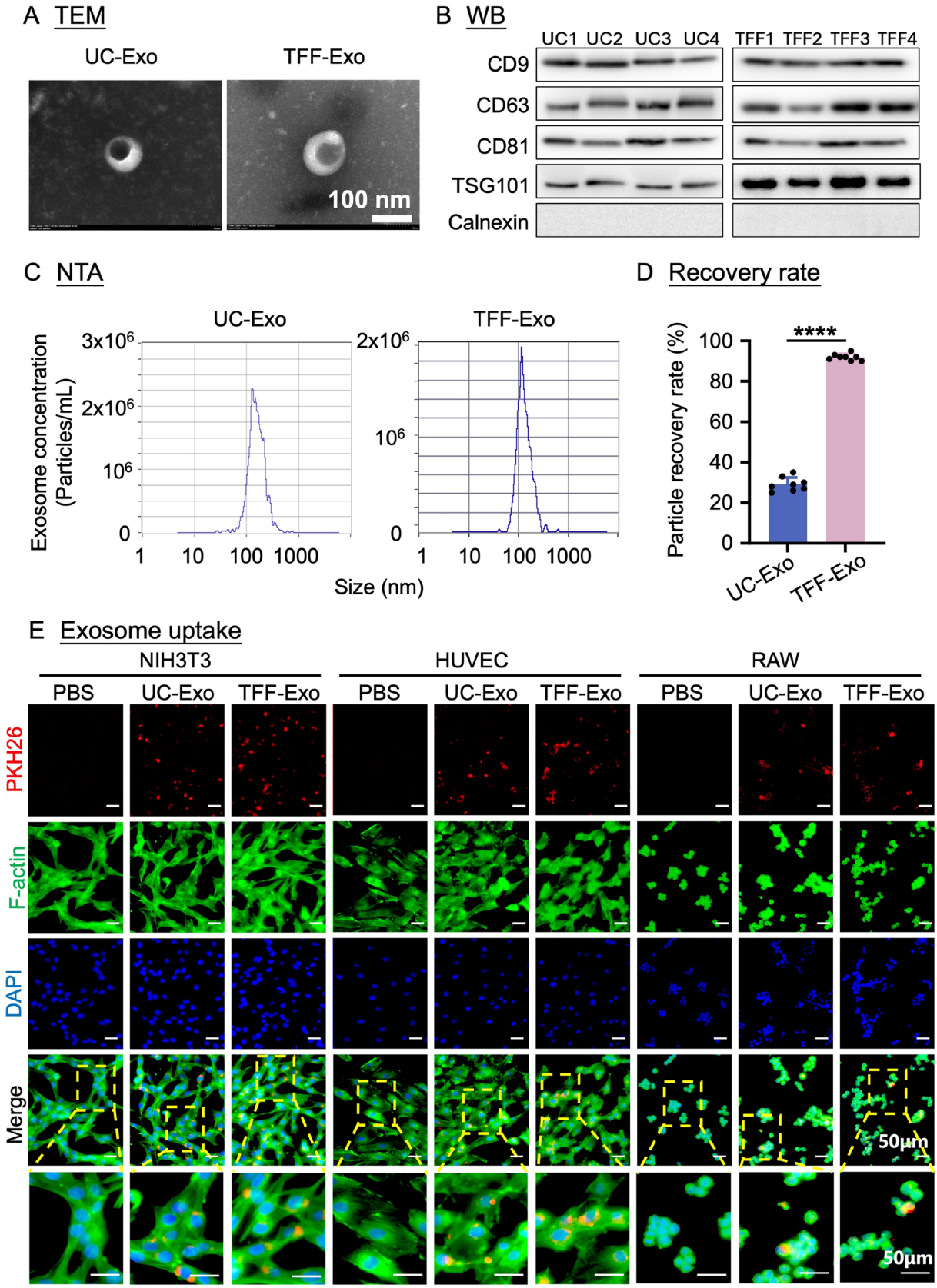

Figure 2. Characterization of ultracentrifugation-isolated exosomes (UC-Exo) and TFF-isolated exosomes (TFF-Exo). (A) Morphology observation by transmission electron microscopy (TEM) analysis: Both UC-Exo and TFF-Exo were cup-shaped or saucer-like particles with well-defined edges. n = 4. (B) Characterization of exosome surface markers using Western blot (WB) analysis: Both UC-Exo and TFF-Exo from four different donors demonstrated expression of positive markers (CD9, CD63, CD81, TSG101) and did not express the negative markers Calnexin. n = 4. (C) Particle size analysis by nanoparticle tracking analysis (NTA): UC-Exo and TFF-Exo showed similar size distribution (100-150 nm). n = 4. (D) Recovery rate: The particle recovery rate of TFF method was 3.2 times higher than that of ultracentrifugation method. The recovery rate is defined as the number of particles remaining in the sample reservoir as a proportion of the initial particles number. n = 8; mean ± SD; ****, $p < 0.0001$. (E) Exosomes uptake by cells: Exosomes labeled with PKH26 were incubated with NIH3T3, HUVECs, and RAW 264.7 cells for 24 h, and the exosome uptake by all these cells was revealed under microscope. Scale bar = 50 μm.

presence of surface markers via TEM, WB, and NTA analyses. TEM images showed that both ultracentrifugation-Exo and TFF-Exo had a typical cup-shaped lipid bilayer morphology with a non-aggregated appearance and clear membrane structures (Figure 2A). WB showed the presence of exosome-specific surface markers CD9, CD63, CD81, and TSG101 in both ultracentrifugation-Exo and TFF-Exo isolated from four different donors, with no expression of calnexin (Figure 2B). NTA revealed that both ultracentrifugation-Exo and TFF-Exo were approximately 100-150 nm in diameter (Figure 2C). Additionally, TFF method demonstrated a threefold increase in recovery rate compared to ultracentrifugation method ($p < 0.05$) with mean recovery rates of 91.88% and 29.13%, respectively (Figure 2D). Herein, HUVECs, NIH-3T3, and RAW 264.7 cells were used as model cell types *in vitro* to evaluate biocompatibility and function of exosomes. To evaluate uptake of exosomes *in vitro*, both ultracentrifugation-Exo and TFF-Exo were labelled by PKH26 and then co-cultured with HUVECs, NIH-3T3, and RAW 264.7 cells separately. As shown in Figure 2E, significant amount of PKH26-labelled exosomes were found to be taken by HUVECs, NIH-3T3, and RAW 264.7 cells after a 24 h co-culture. Collectively, these data showed successful isolation of high-quality exosomes using the TFF method that met the standard of MISEV guidelines,[1] with a significantly higher extraction yield compared to the ultracentrifugation extraction method.

3.2. Ultracentrifugation-Exo and TFF-Exo were biocompatible and enhanced cell migration in vitro

The viability of HUVECs and NIH-3T3 cells co-cultured with either ultracentrifugation-Exo or TFF-Exo was evaluated using Calcein-AM/PI staining and the CCK-8 assay (Figure 3A). Compared with untreated control, both ultracentrifugation-Exo and TFF-Exo treated HUVECs and NIH-3T3 cells exhibited similar cell viability, with no statistically significant differences observed, indicating the biocompatibility of both exosome preparations. In addition, the effects of ultracentrifugation-Exo or TFF-Exo on the migratory activity of HUVECs were assessed by scratch and Transwell migration assays. Results from the scratch assay demonstrated that the migratory ability of HUVECs cultured with either ultracentrifugation-Exo or TFF-Exo was enhanced compared to the untreated control group. Specifically, the ratio of the scratch area of HUVECs was significantly reduced after treatment with either ultracentrifugation-Exo (37.30%) or TFF-Exo (30.60%) ($p < 0.05$), compared to the untreated control group (83.69%), with no significant difference observed between the two exosome-treated groups (Figure 3B). The results of Transwell migration assay were consistent with those from the scratch assay, as ultracentrifugation-Exo and TFF-Exo treatment significantly increased the migratory activity of HUVECs compared to untreated control ($p < 0.05$) (Figure 3C). Taken together, these results indicated that both ultracentrifugation-Exo and TFF-Exo are biocompatible and promote cell migration.

3.3. Ultracentrifugation-Exo and TFF-Exo exhibited pro-angiogenic and anti-inflammatory effects in vitro

Numerous studies have shown that exosomes promote angiogenesis and influence immune regulation.[1] In this study, the pro-angiogenesis effects of ultracentrifugation-Exo and TFF-Exo were evaluated in cultured HUVECs using a tube formation assay. Compared to the untreated control group, both ultracentrifugation-Exo and TFF-Exo induced phenotypic changes in HUVECs, resulting in an increased formation of vascular structures, as evidenced by the increased number of nodes and branches ($p < 0.05$) (Figure 4A). No significant differences were observed between the ultracentrifugation-Exo and TFF-Exo groups. Moreover, to assess the effect of ultracentrifugation-Exo and TFF-Exo on inflammatory modulation, M0 macrophages were initially polarized into M1 type macrophages using LPS. After successful induction, M1 macrophages were further treated with either ultracentrifugation-Exo or TFF-Exo, while untreated M1 macrophages served as the control. After 24 hours of incubation, flow cytometry analysis was conducted to assess the extent of macrophage polarization. While only a small amount of M2 macrophages were produced in the untreated group (9.61% of M2 macrophages), in contrast treatment with ultracentrifugation-Exo and TFF-Exo groups resulted in production of approximately 28.17% and 31.14% M2 macrophages, respectively, suggesting that both ultracentrifugation-Exo and TFF-Exo effectively promoted the transition of macrophages toward the M2 phenotype and showed potential anti-inflammatory efficacy (Figure 4B). Taken together, these findings demonstrate that TFF-Exo possess pro-angiogenic and anti-inflammatory efficacy comparable to that of ultracentrifugation-Exo.

3.4. Ultracentrifugation-Exo and TFF-Exo enhanced wound repair in a mouse diabetic model

The therapeutic effect of ultracentrifugation-Exo and TFF-Exo on wound healing was assessed using a full-thickness skin defect model in diabetic mice. One week after STZ treatment, 0.1 mL physiological saline (serving as control group), ultracentrifugation-Exo, or TFF-Exo (1×10^{10} particles in 0.1 mL physiological saline) were injected subcutaneously around the wound areas. Both ultracentrifugation-Exo and TFF-Exo were labelled with the near-infrared fluorescence tracer DiR to track their distribution *in vivo*. As depicted in Figure 5A, mice were optically imaged 3, 12, and 24 hours after subcutaneous injection of exosomes. Compared with the physiological saline group, DiR-labelled ultracentrifugation-Exos and TFF-Exos were observed in the wound site after subcutaneous injection, and a stable and clear fluorescent signal was achieved after 3 hours and continued to 24 hours. Additionally, a similar distribution pattern was observed in both the ultracentrifugation-Exo and TFF-Exo groups.

Morphometric observations of the percentage of wound closure at days 3, 6, and 9 showed that wound healing was slower in the control group compared to the exosomes treatment groups as the residual wound areas were significantly reduced in both the ultracentrifugation-Exo and TFF-Exo groups compared to physiological saline injection ($p < 0.05$) (Figure 5B). Subsequently, wound healing was evaluated histologically to assess the therapeutic consequences of different interventions. H&E staining demonstrated that, compared to the control group, the ultracentrifugation-Exo- and TFF-Exo-treated wounds were filled with more abundant newly formed granulation tissue along with an increased epidermal thickness and more pronounced re-epithelization of the wound bed (Figure 5C). Additionally, Masson's trichrome staining revealed that the exosome-treated groups had thicker and denser collagen

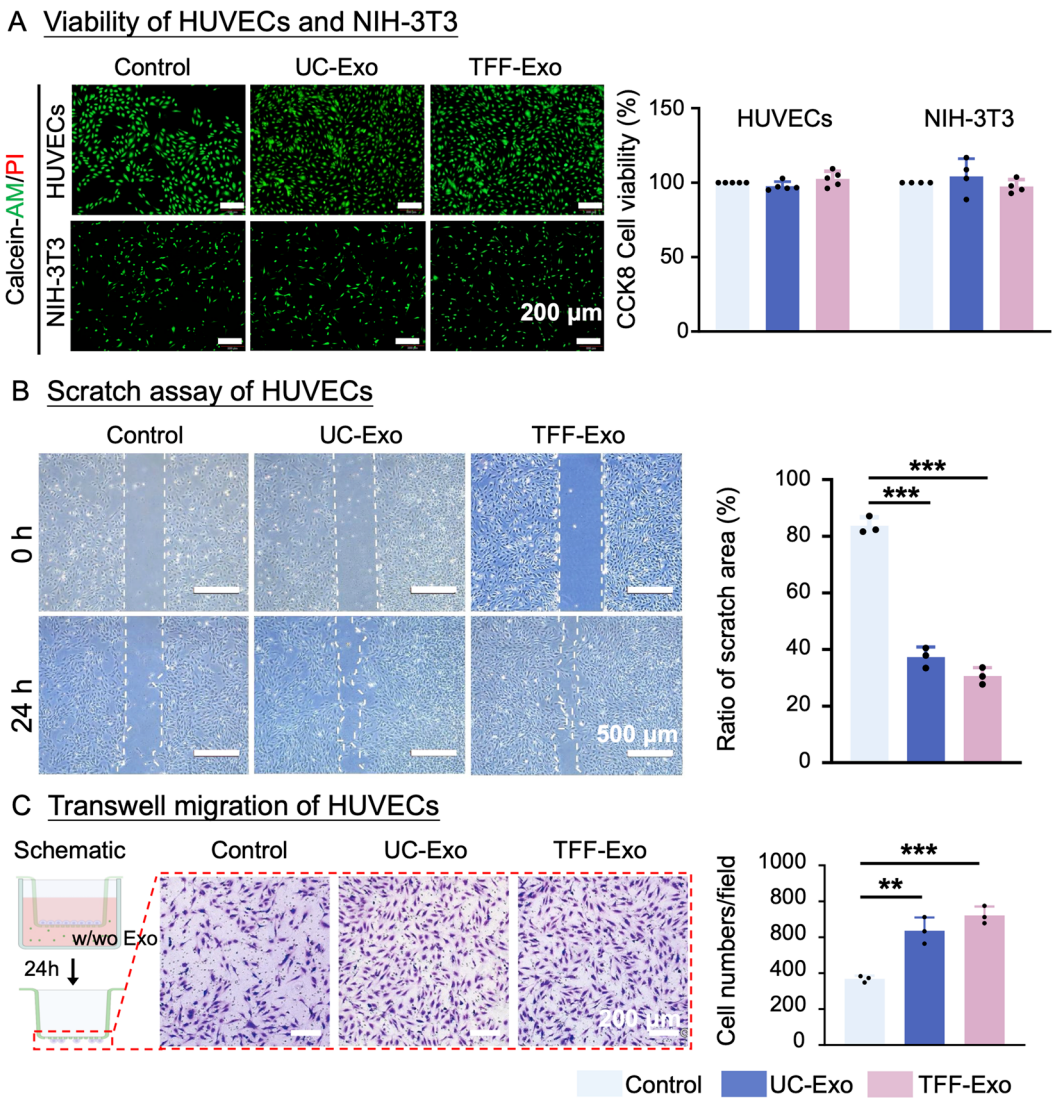

Figure 3. *In vitro* assessment of cell viability and cell migration in exosome-containing medium. (A) Cell viability detection by calcein-AM/PI staining and the CCK-8 assay: High viability of HUVECs and fibroblasts were observed in both UC-Exo and TFF-Exo groups, demonstrating biocompatibility of TFF-Exo and UC-Exo. Scale bar = 200 μm. (B) Cell migration analysis using the scratch wound assay: The similar residual wound area of HUVECs in UC-Exo or TFF-Exo group, which was significantly smaller than that of the control group, indicates that UC-Exo and TFF-Exo can promote the migratory ability of HUVECs. Scale bar = 500 μm. (C) Cell migration assay using the transwell assay: Higher cell density on the bottom side of the transwell insert in the UC-Exo and TFF-Exo groups further demonstrated that UC-Exo and TFF-Exo promoted the migratory ability of HUVECs. Scale bar = 200 μm. ($n = 3$ biological replicates, mean ± *SD*; **, $p < 0.01$; ***, $p < 0.001$.).

fibers, characterized by a deep blue staining coloration indicative of enhanced collagen deposition, whereas the control group showed weaker collagen staining results (Figure 5C). These observations showed that both ultrecentrifugation-Exo and TFF-Exo demonstrated effective therapeutic benefits in promoting wound healing in diabetic mice.

3.5. Ultracentrifugation-Exo and TFF-Exo promoted angiogenesis and anti-inflammatory effects in a mouse diabetic wound healing model

The *in vivo* diabetic wound healing model was also used to assess the pro-angiogenic and anti-inflammatory effects of ultracentrifugation-Exo and TFF-Exo via IHC and IF staining as well as RT-qPCR analysis.

Neovascularization, identified by the presence of CD31-positive vascular endothelial cells, was observed in the newly formed skin at the wound site on day 9 in all groups. Morphometrtic analysis of CD31-positive area in the wound tissue revealed that the number of newly formed blood vessels in both ultracentrifugation-Exo- and TFF-Exo-treated groups were significantly higher compared to the control group, with no significant difference between the ultracentrifugation-Exo and TFF-Exo groups ($p < 0.05$) (Figure 6A-B). The results of IF staining for α-SMA were consistent with those from CD31 staining. Quantitative analysis showed that the number of α-SMA positive cells was significantly higher in both ultracentrifugation-Exo- and TFF-Exo-treated groups compared to the control group ($p < 0.05$) (Figure 6C-D). In addition, on day 9, the mRNA expression levels of angiogenesis-related factors (PDGF, HIF-1α) and fibroblast activation markers (Collagen I) were significantly higher in the diabetic wounds treated with ultracentrifugation-Exo or

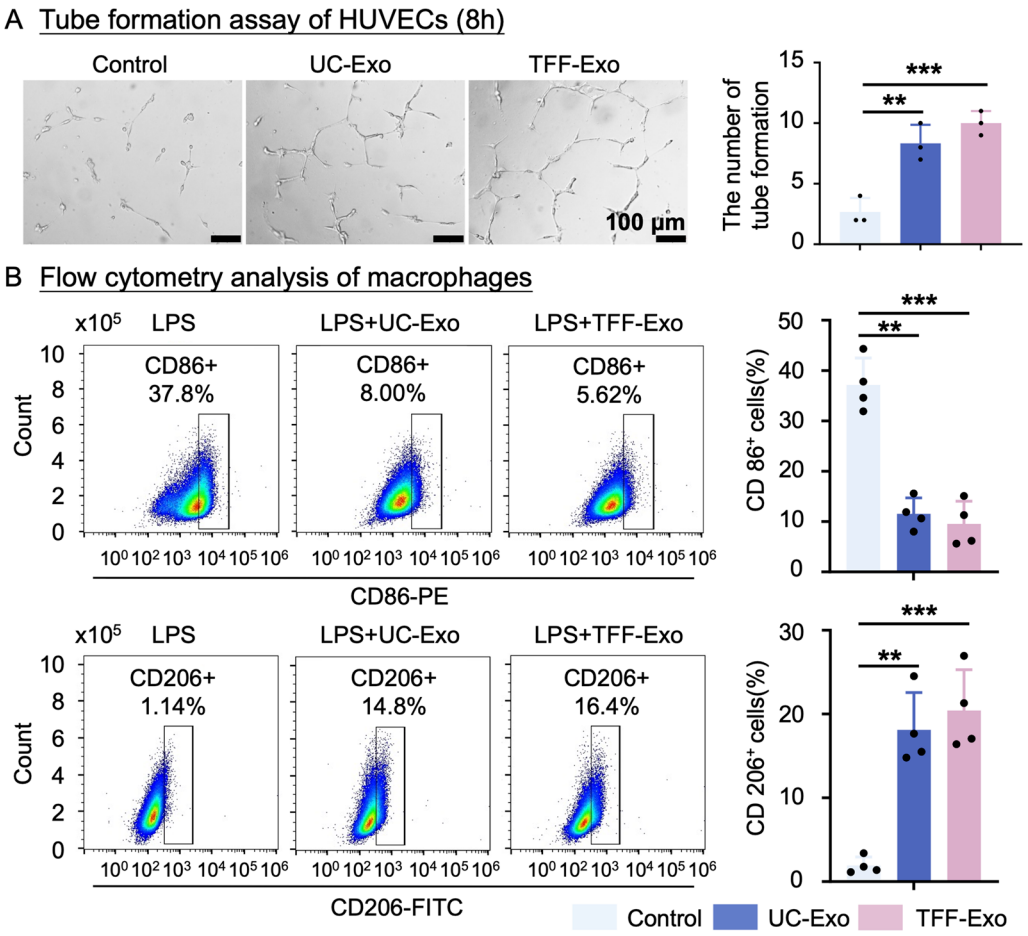

Figure 4. *In vitro* assessment of the angiogenic and immunomodulatory capacities of UC-Exo and TFF-Exo. (A) Tube formation assay of HUVECs: The tube formation of HUVECs were significantly increased in UC-Exo and TFF-Exo group compared to the control group, which indicates the pro-angiogenic abilities of UC-Exo and TFF-Exo. Scale bar = 100 μm. (B) Detection of CD86 and CD206 on F4/80+ cells using flow cytometry: Both UC-Exo and TFF-Exo significantly upregulated the ratio of CD206+ macrophages and downregulated the ratio of CD86+ macrophages compared to LPS, indicating that they possess strong immunomodulatory capacities by promoting M2 polarization and inhibiting M1 polarization of macrophages. ($n = 3$ biological replicates, mean ± *SD*; **, $p < 0.01$, ***, $p < 0.001$.).

TFF-Exo compared to the control group ($p < 0.05$) (Figure 6E). These data suggest that both ultracentrifugation-Exo and TFF-Exo exhibit pro-angiogenic effects, enhancing capillary formation and fibroblast activation.

Paracrine signaling of M1-polarized macrophages is one of the key factors contributing to endothelial cell and fibroblast dysfunction in diabetic wound healing.[30] We quantified mRNA levels of pro- and anti-inflammatory cytokines using RT-qPCR. The results showed that on day 9, compared to the control group, the exosome-treated groups exhibited significantly reduced expression levels of proinflammatory cytokines (IL-1β, TNF-α, and iNOS2) and increased expression levels of anti-inflammatory cytokines (CD163, CD206, and TGF-β) ($p < 0.05$). Notably, the TFF-Exo group exhibited significantly lower IL-1β mRNA expression levels, and higher CD206 mRNA expression levels compared to the ultracentrifugation-Exo group ($p < 0.05$) (Figure 7A). Moreover, macrophage polarization in the wound tissue was further investigated using IF staining. Quantitative analysis of macrophages in the wound tissue showed that the exosome-treated groups displayed significantly lower protein levels of the M1-polarized macrophage marker iNOS2 and higher protein levels of the M2-polarized macrophage marker CD206 compared to the physiological saline group ($p < 0.05$) (Figure 7B). These findings suggested that both ultracentrifugation-Exos and TFF-Exos can mitigate inflammation by enhancing M2 macrophage polarization.

Taken together, these results highlight that both ultracentrifugation-Exo and TFF-Exo treatment may potentially promote angiogenesis and modulate the inflammatory response by enhancing M2-type macrophage polarization in diabetic wound healing in mice.

4. Discussion

In this study, we characterized TFF-Exo and ultracentrifugation-Exo and compared them based on quality and therapeutic efficacy, particularly in the context of diabetic wound healing *in vivo*. Our results demonstrated that the TFF method successfully isolated high-quality exosomes which meet the standard of MISEV guidelines,[1] with a significantly higher extraction yield compared to the traditional ultracentrifugation extraction method. Moreover, both TFF-Exo and ultracentrifugation-Exo exhibited similar biological activity *in vitro*, as well as comparable therapeutic potential for the treatment of diabetic wounds *in vivo*. Furthermore, this healing effect is potentially facilitated through mechanisms involving angiogenesis and macrophage polarization.

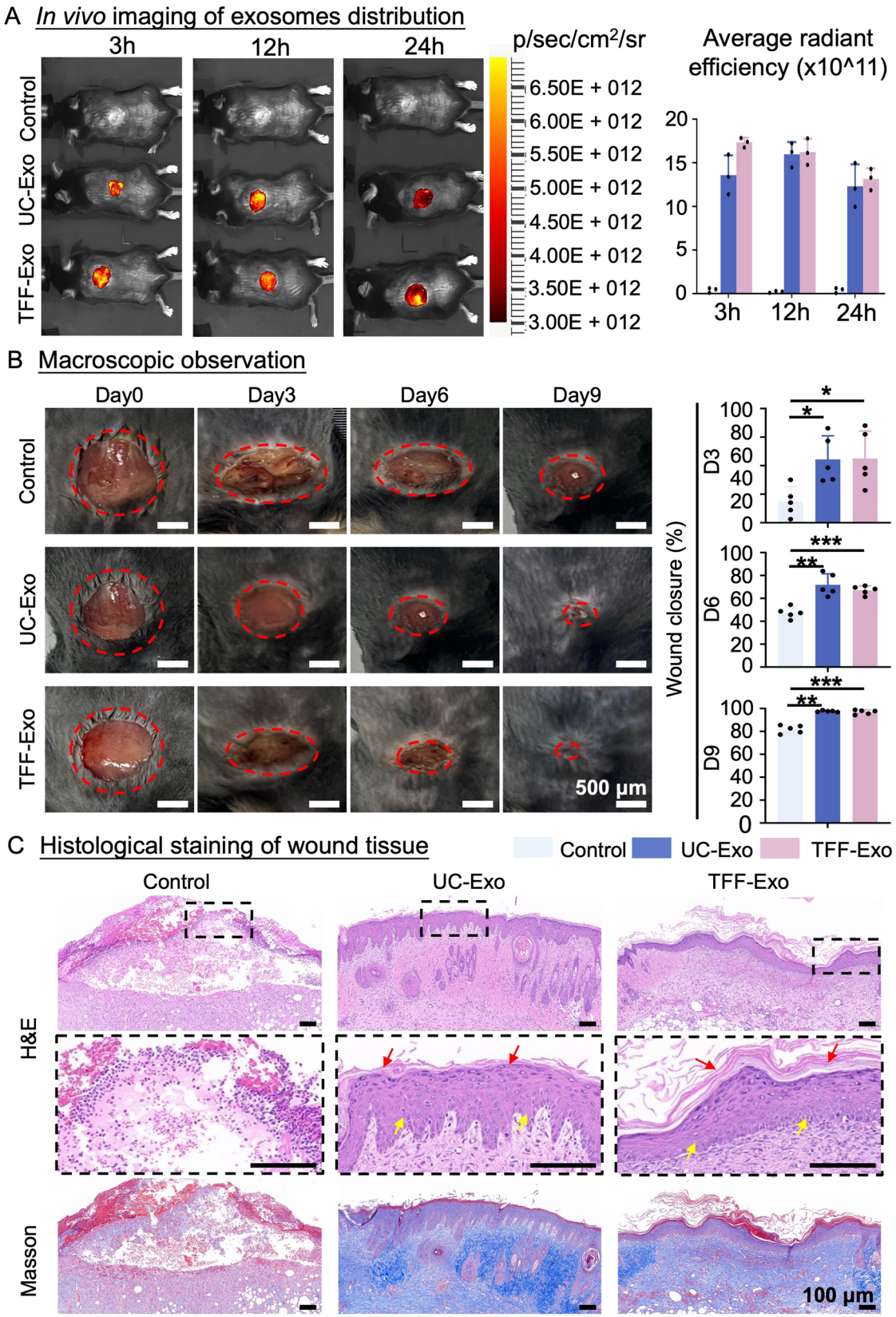

Figure 5. Macroscopic and histological assessment of the effect of UC-Exo and TFF-Exo for diabetic wound repair in mice. (A) Time-dependent images and semiquantitative analysis of DiR-labelled UC-Exo and TFF-Exo in mice ventral views: Both UC-Exo and TFF-Exo were locally retained and enriched in the subcutaneous tissue at the injection site at 3 h, 12 h, and 24 h after the treatment. $n = 3$. (B) Light field photographs of skin wound healing process: A smaller wound area was observed in UC-Exo and TFF-Exo groups compared tophysiological saline group at 3, 6, and 9 days post-treatment. The red dotted circle indicates the area of skin defect. $n = 5$, mean ± *SD*; *, $p < 0.05$; **, $p < 0.01$; ***, $p < 0.001$. (C) Histological evaluation of diabetic wound promoted by UC-Exo and TFF-Exo: The H&E staining showed abundant newly formed granulation tissue (yellow arrow) and neo-epidermis (red arrow) in UC-Exo and TFF-Exo groups compared to physiological saline group. Masson's trichrome staining demonstrated thicker and denser collagen fibers (blue staining) in the UC-Exo and TFF-Exo groups relative to the physiological saline group. Scale bar = 200 μm.

Our previous study reported enhanced therapeutic effects of 3D-cultured hUCMSCs on diabetic wound healing compared to 2D-cultured hUCMSCs.[24] Therefore, in this study, we aim to investigate the therapeutic effects of exosomes derived from the 3D-cultured hUCMSCs, as a cell-free therapy, for the clinical translation of diabetic wound healing. Ultracentrifugation is currently considered the gold standard protocol for exosome extraction due to its effectiveness in removing impurities and its capability to process relatively large volumes (up to 1.5 L). However, the isolated exosomes can aggregate and precipitate alongside protein aggregates and other non-exosome particles.[17] TFF is a relatively gentle, size-based fractionation method that minimizes exosome aggregation and can efficiently process scalable volumes of biological fluids, making it both time- and cost-effective.[17] For clinical applications, however, further characterization of the quality and therapeutic efficacy of the TFF-Exo is essential. Therefore, we benchmarked the efficiency of the TFF isolation method against ultracentrifugation and investigated the therapeutic effects of TFF-Exo for diabetic wound repair. In this study, standard identification methods, ie, TEM, NTA, and WB analysis, were employed to characterize TFF-Exo and ultracentrifugation-Exo, both of which were found to meet the standard criteria for exosomes as described by Welsh et al.[32] Notably, the TFF system achieved a higher recovery rate than ultracentrifugation, resulting in greater yields from the same volume of cell culture medium. This is attributed to TFF's cross-flow filtration principle, which prevents molecular accumulation and membrane fouling.[17] Additionally, TFF reduces yield loss from filter plugging and minimizes damage to exosome integrity caused by high-speed centrifugation.[17,33] Thus, based on these findings, TFF emerges as a reliable and efficient alternative to the traditional ultracentrifugation method for clinical translation.

Ultracentrifugation-Exo has shown significant therapeutic effects on diabetic wound healing *in vivo* by promoting angiogenesis and inducing anti-inflammatory macrophages.[23,34,35] Our result showed that both ultracentrifugation-Exo and TFF-Exo can be taken up by recipient cells *in vitro*, including

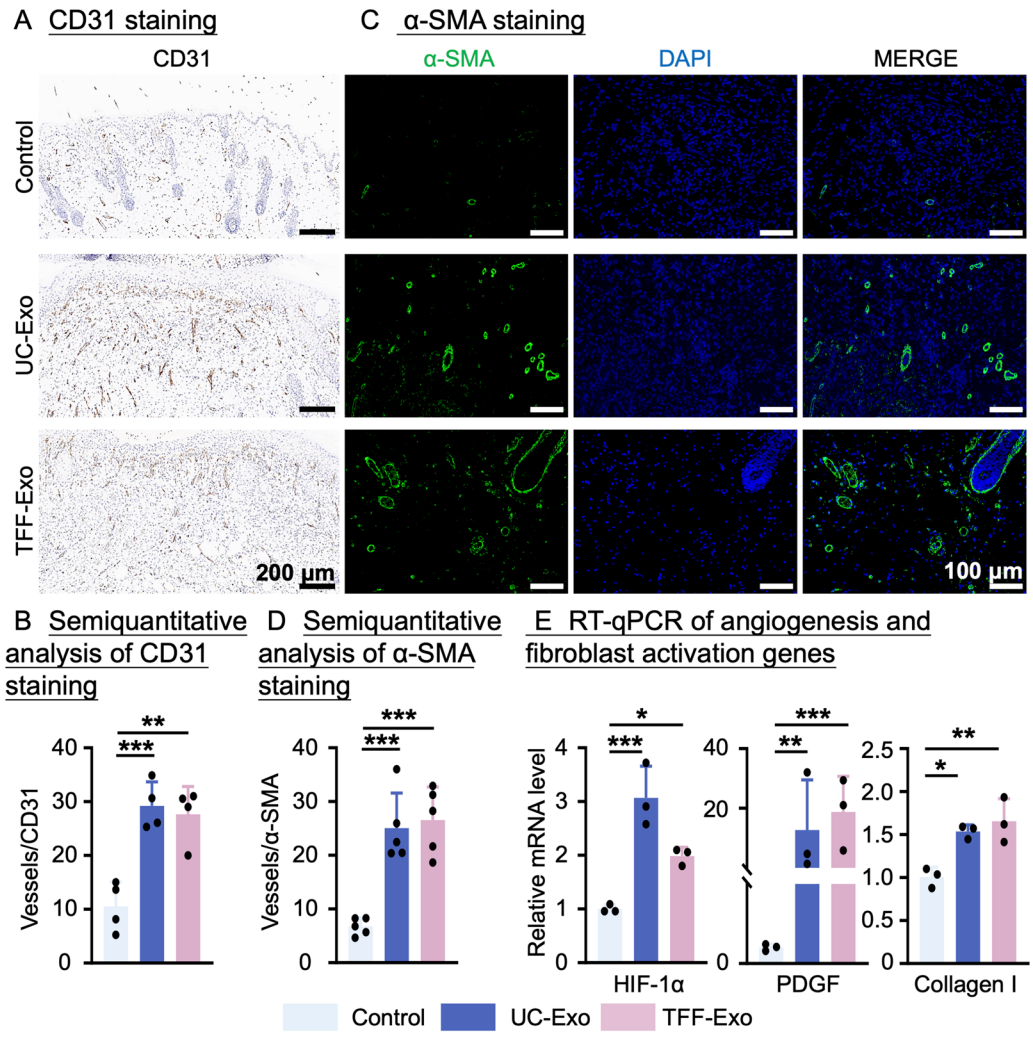

Figure 6. Assessment of *in vivo* angiogenesis in diabetic wound healing promoted by UC-Exo and TFF-Exo. (A-B) IHC staining of the pro-angiogenic protein (CD31) and its semi-quantitative analysis: The UC-Exo and TFF-Exo groups demonstrated a higher expression level of CD31 compared to the physiological saline group. Scale bar = 200 μm. (C-D) IF staining of the angiogenesis-related protein (α-SMA) and its semi-quantitative analysis: The UC-Exo and TFF-Exo groups showed a stronger fluorescent signal of α-SMA compared to physiological saline group. Scale bar = 100 μm. (E) RT-qPCR analysis: The UC-Exo and TFF-Exo groups exhibited higher expression levels of genes associated with angiogenesis and fibroblast activation (HIF-α, PDGF, and Collagen I) compared to physiological saline group. ($n = 4$, mean ± SD; *, $p < 0.05$; **, $p < 0.01$; ***, $p < 0.001$.).

HUVECs (Figure 2). Additionally, the endothelial tube formation assay demonstrated similar pro-angiogenic capacities for both ultracentrifugation-Exo and TFF-Exo groups. These results are in accordance with results from previous research demonstrating the biocompatibility and the angiogenic potential of exosomes extracted from MSCs.[36,37] Specifically, MSC-derived exosomes have been reported to enhance the migration, proliferation, and blood vessel regeneration potential of vascular endothelial cells.[38] *In vivo* tracking confirmed the presence of both ultracentrifugation-Exo and TFF-Exo at the wound site post-injection. Both treatments significantly upregulated the expression of angiogenic markers compared to control, validating the robust pro-angiogenic effect of both exosome preparations on wound healing. The gene expression levels of HIF-1α and PDGF were quantified, along with positive staining for CD31 and α-SMA, within the diabetic wound tissue. HIF-1α and PDGF have been reported to be involved in facilitating vascularization and granulation tissue formation, leading to accelerated wound regeneration,[39,40] while CD31 and α-SMA are markers for detecting newly formed vessels and mature vessels, respectively.[41] Hu et al. demonstrated that exosomes derived from bone marrow-derived MSCs enhanced the expression of CD31, thereby facilitating adequate angiogenesis in the context of diabetic wound healing.[42] Yu et al., also highlighted that MSC-extracted exosomes promoted the formation and maturation of blood vessels at wound sites, as evidenced by increased IF staining intensity for the CD31 and α-SMA markers.[40] Taken together, our findings demonstrate that exosomes significantly enhance endothelial cell migration and angiogenesis *in vitro* and *in vivo*

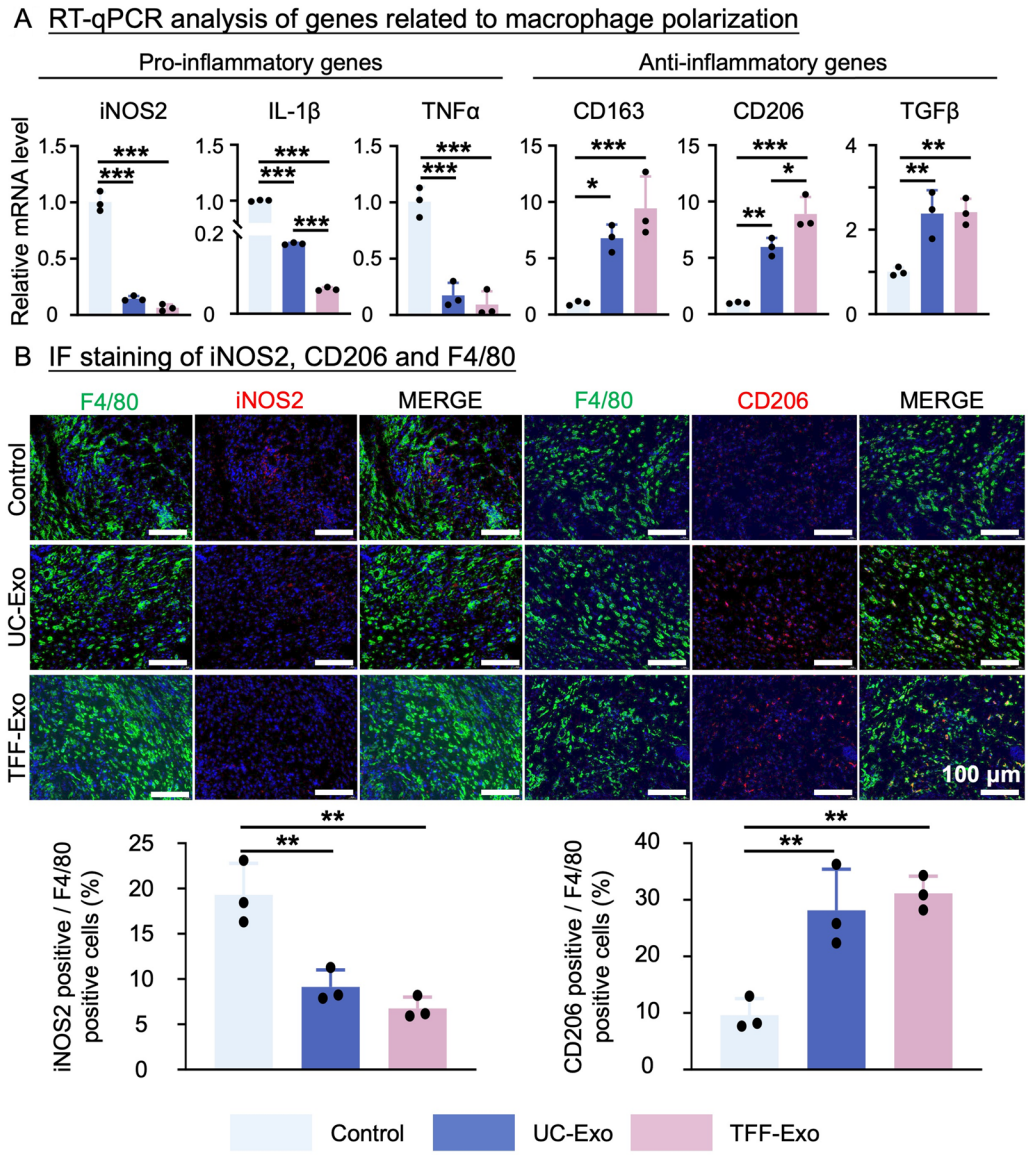

Figure 7. Assessment of the anti-inflammatory effects of UC-Exo and TFF-Exo for diabetic wound healing in mice. (A) RT-qPCR of genes associated with macrophage polarization: The UC-Exo and TFF-Exo groups revealed a lower expression level of pro-inflammatory genes (iNOS2, IL-1β, and TNF-α) and higher expression level of anti-inflammatory genes (CD163, CD206, and TGF-β) compared to the physiological saline group. (B) Detection of proteins associated with macrophage polarization using IF staining: The UC-Exo and TFF-Exo groups showed a weaker signal of typical marker protein of M1 macrophage (iNOS2) and enhanced signal of typical marker protein of M2 macrophage (CD206) compared to the physiological saline group. Scale bar = 100 μm. ($n = 3$, mean ± *SD*; *, $p < 0.05$; **, $p < 0.01$; ***, $p < 0.001$.)

through paracrine mechanisms promoting neovascularization and collagen deposition in the wound bed, thereby accelerating diabetic wound healing.

Next, the effects of the exosome on the anti-inflammatory response in diabetic wound healing *in vivo* were evaluated (Figure 7). Recent studies have highlighted the critical role of macrophage polarization in the inflammatory processes associated with diabetic wound healing.[43–45] Macrophages as pioneer immune cells play a distinct and vital role in the different stages of wound repair. Pro-inflammatory M1 macrophages can promote inflammation via the secretion of TNF-α and other inflammatory factors, while M2 phenotypes can elicit anti-inflammatory activities.[46,47] Notably, published studies suggested that increasing the amount of M2 macrophages and decreasing the amount of M1 macrophages were conductive to diabetic wounds repair.[48,49] In this study, the anti-inflammatory effects of exosomes on macrophages were further explored. Our *in vitro* data revealed that exosomes could promote immune modulation by inducing M2 macrophage polarization. In the *in vivo* diabetic wound model, both ultracentrifugation-Exo and TFF-Exo effectively enhanced wound healing by modulating macrophage polarization and inflammation. Notably, IL-1β levels decreased more significantly following treatment with TFF-Exo compared to ultracentrifugation-Exo. Moreover, the upregulation of M2 polarization related gene expression in both exosomes treated groups was noted, with higher CD206 expression in TFF-Exo groups compared to ultracentrifugation-Exo. The statistically significant increase in the ratio of positive staining of CD206 to F4/80 (pan macrophage marker) in the both exosome groups compared to the control further supported the role of exosomes in promoting M2 macrophage polarization, consistent with previous findings.[50,51] Moreover, Liu et al. showed that exosomes secreted by MSCs and isolated by ultracentrifugation inhibited M1 polarization and promoted M2 polarization, thereby reducing inflammation and enhancing skin wound healing.[52] These results suggest that both ultracentrifugation-Exo and TFF-Exo can regulate immune responses and exert anti-inflammatory effects.

Based on our results regarding angiogenesis and anti-inflammation, no difference in bioactivity and effectiveness could be observed between ultracentrifugation-Exo and TFF-Exo. Similar results can be found in the literature, where Watson at al. indicated no significant differences in the content of bioactive molecules between TFF-Exo and ultracentrifugation-Exo.[53] Meanwhile, the study by Haraszti et al., suggested that TFF-Exo are seven times more effective in small interfering RNA transfer to neurons than ultracentrifugation-Exo.[18] Additionally, a study by Kim et al. demonstrated that TFF-Exo exhibited higher levels of the angiogenic marker proteins HGF, angiopoietin-1, and bFGF compared to ultracentrifugation-Exo.[16] However, the variations in experimental conditions and cell sources employed in these studies limit direct comparisons between these findings. Therefore, further comprehensive investigations with standardized settings are necessary to elucidate the differences in bioactivity and efficacy between ultracentrifugation-Exo and TFF-Exo.

Interestingly, our current study, utilizing TFF-Exo derived from 3D cultured hUCMSCs, achieved a similar outcome in diabetic wound healing compared to our previous study, which immediately used 3D cultured hUCMSCs. This was evidenced by comparable wound closure rates and histological staining results.[24] This suggests that exosomes can effectively harness the regenerative potential of hUCMSCs while circumventing the complexities associated with traditional cell therapies. Moreover, to enhance wound repair, the quantity of cells used for exosome isolation via ultracentrifugation in this study was similar to that used in our earlier research for *in vivo* cell injections (1 × 10^6 cells/mouse).[24] This aligns with literature report indicating that cell quantity required for effective wound repair is around 1 × 10^5 to 2 × 10^6 cells per wound in rodent models.[54] In contrast, using the TFF isolation approach required 5 to 10 times fewer cells to achieve the same yield of exosomes and therapeutic effectiveness (data not shown). Thus, our findings suggest that exosomes isolated using the TFF method achieve comparable therapeutic effects while requiring significantly fewer donor cells in a 3D biofabrication system, offering a more cost-effective approach. By showcasing the significant therapeutic effects of exosomes isolated from 3D-cultured hUCMSCs by the scalable TFF method, this study emphasizes the potential of exosome-based therapies as an industrialized and translational strategy to enhance wound healing.

There are some limitations in our study. First, the choice of stem cell sources for exosome production is contingent upon the specific type of disease.[55] For example, Zhu et al. demonstrated that exosomes from induced pluripotent stem cells-derived MSC could provide a stronger therapeutic effect on osteoarthritis than synovial membrane MSC-derived exosomes.[56] However, our study only utilized hUCMSCs as a representative example to produce exosomes using TFF and ultracentrifugation methods. Therefore, further characterization with exsomes derived from other cell sources is required to establish the universality of the exceptional TFF isolation system. Secondly, further characterization of the exosome production environment at Good Manufacturing Practice levels is necessary for the industrialization and clinical application of exosomes isolated with the TFF system.[20] These limitations will be addressed in future research.

5. Conclusion

In conclusion, this study demonstrated the capacity of TFF to produce large quantities of exosomes that meet the quality and safety standard requirements. Both *in vivo* and *in vitro* experiments confirmed that TFF-Exo exhibit functionality and efficacy similar to ultracentrifugation-Exo. Under current conditions, the large-scale preparation using the TFF method yields higher quantities compared to traditional ultracentifugation methods, suggesting that TFF-Exo may offer significant advantages for future cell-free therapy, particularly in wound healing-related conditions in clinical settings.

Author contributions

Yanmei Chen: Collection and/or assembly of data, manuscript writing and editing

Yang Xu: Data analysis and interpretation, manuscript writing and editing

Yali Zheng: Collection and/or assembly of data

Yingda Yan, Jiawei Cai, Chu Hua, Jiang Li, Cheng Zhang: Collection and/or assembly of data

Marianne Lauwers, Ying Rao, Zhenyu Zhong: Manuscript writing and editing

Dai Fei Elmer Ker, Rocky S. Tuan: Manuscript writing and editing, financial support, final approval of manuscript

Xiao Yang: Conception and design, final approval of manuscript

Dan Michelle Wang: Conception and design, manuscript writing and editing, financial support, final approval of manuscript

Zhiyong Zhang: Conception and design, manuscript writing and editing, financial support, final approval of manuscript

Ethics statement

The present study was approved by the Institutional Ethics Review Board of the Third Affiliated Hospital of Guangzhou Medical University and Guangdong Provincial Medical Laboratory Animal Center. (Ethics number: human: 2020_001, animal: G2024-1255).

Funding

This work was supported by Guangdong Basic and Applied Basic Research Foundation [No. 2023B1515130006, ZZ], National Natural Science Foundation of China [No. 82072415, ZZ], Regulatory Science Research Project of the Greater Bay Area Sub-Center for Drug Evaluation and Inspection of National Medical Products Administration [No. GBA-JGKX-2404, ZZ]. This study was funded in part by the InnoHK initiative of the Innovation and Technology Commission of the Hong Kong Special Administrative Region Government (DFEK, RST, and DMW).

Conflict of interest

Zhiyong Zhang is a scientific advisor for REGEN-αGEEK Biotechnology CO., LTD. Cheng Zhang is an employee of REGEN-αGEEK Biotechnology CO., LTD. The authors have no commercial, proprietary, or financial interest in the products or companies described in this article. All other co-authors declare no competing interests.

Data availability statement

The datasets generated during and/or analyzed during the current study are available from the corresponding author upon reasonable request.

References

1. Welsh JA, Goberdhan DCI, O'Driscoll L, et al. Minimal information for studies of extracellular vesicles (MISEV2023): from basic to advanced approaches. *J Extracell Vesicles*. 2024;13:e12404.
2. Yan W, Li Y, Xie S, et al. Chondrocyte-targeted delivery system of sortase A-engineered extracellular vesicles silencing MMP13 for osteoarthritis therapy. *Adv Healthc Mater*. 2024;13:e2303510.
3. Shi L, Zhou Y, Yin Y, et al. Advancing tissue damage repair in geriatric diseases: Prospects of combining stem Cell-Derived exosomes with hydrogels. *Int J Nanomed*. 2024;19:3773-3804.
4. Kim YJ, Yoo SM, Park HH, et al. Exosomes derived from human umbilical cord blood mesenchymal stem cells stimulates rejuvenation of human skin. *Biochem Biophys Res Commun*. 2017;493:1102-1108.
5. Zhu Z, Zhang X, Hao H, et al. Exosomes derived from umbilical cord mesenchymal stem cells treat cutaneous nerve damage and promote wound healing. *Front Cell Neurosci*. 2022;16:913009.
6. Furuta T, Miyaki S, Ishitobi H, et al. Mesenchymal stem cell-derived exosomes promote fracture healing in a mouse model. *Stem Cells Transl Med*. 2016;5:1620-1630.
7. Huang S, Rao Y, Zhou M, et al. Engineering an extracellular matrix-functionalized, load-bearing tendon substitute for effective repair of large-to-massive tendon defects. *Bioact Mater*. 2024;36:221-237.
8. Zhang W, Rao Y, Wong SH, et al. Transcriptome-Optimized hydrogel design of a stem cell niche for enhanced tendon regeneration. *Adv Mater*. 2025;37:e2313722.
9. Yang X, Cheung YMC, Liling L, et al. Optimizing biophysical properties of cellular niches to enhance stem cell-derived extracellular vesicle function in musculoskeletal regeneration. *BMEMat*. 2025; e70012.
10. Kimiz-Gebologlu I, Oncel SS. Exosomes: Large-scale production, isolation, drug loading efficiency, and biodistribution and uptake. *J Control Release*. 2022;347:533-543.
11. Gardiner C, Di Vizio D, Sahoo S, et al. Techniques used for the isolation and characterization of extracellular vesicles: results of a worldwide survey. *J Extracell Vesicles*. 2016;5:32945.
12. Royo F, Théry C, Falcón-Pérez JM, Nieuwland R, Witwer KW. Methods for separation and characterization of extracellular vesicles: results of a worldwide survey performed by the ISEV rigor and standardization subcommittee. *Cells*. 2020;9:1955.
13. Huang S, Rao Y, Ju AL, et al. Non-collagenous proteins, rather than the collagens, are key biochemical factors that mediate tenogenic bioactivity of tendon extracellular matrix. *Acta Biomater*. 2024;176:99-115.
14. Lai JJ, Chau ZL, Chen S-Y, et al. Exosome processing and characterization approaches for research and technology development. *Adv Sci*. 2022;9:2103222.
15. Williams S, Fernandez-Rhodes M, Law A, Peacock B, Lewis MP, Davies OG. Comparison of extracellular vesicle isolation processes for therapeutic applications. *J Tissue Eng*. 2023;14:20417314231174609.
16. Kim JY, Rhim WK, Yoo YI, et al. Defined MSC exosome with high yield and purity to improve regenerative activity. *J Tissue Eng*. 2021;12:20417314211008626.
17. Visan KS, Lobb RJ, Ham S, et al. Comparative analysis of tangential flow filtration and ultracentrifugation, both combined with subsequent size exclusion chromatography, for the isolation of small extracellular vesicles. *J Extracell Vesicles*. 2022;11:e12266.
18. Haraszti RA, Miller R, Stoppato M, et al. Exosomes produced from 3D cultures of MSCs by tangential flow filtration show higher yield and improved activity. *Mol Ther*. 2018;26:2838-2847.
19. Bae JH, Lee CH, Jung D, et al. Extracellular vesicle isolation and counting system (EVics) based on simultaneous tandem tangential flow filtration and large field-of-view light scattering. *J Extracell Vesicles*. 2024;13:e12479.
20. Ma CY, Zhai Y, Li CT, et al. Translating mesenchymal stem cell and their exosome research into GMP compliant advanced therapy products: promises, problems and prospects. *Med Res Rev*. 2024;44:919-938.
21. Song Y, You Y, Xu X, et al. Adipose-derived mesenchymal stem cell-derived exosomes biopotentiated extracellular matrix hydrogels accelerate diabetic wound healing and skin regeneration. *Adv Sci (Weinh)*. 2023;10:e2304023.
22. Armstrong DG, Tan TW, Boulton AJM, Bus SA. Diabetic foot ulcers: a review. *JAMA*. 2023;330:62-75.
23. Lazzarini PA, Cramb SM, Golledge J, Morton JI, Magliano DJ, Van Netten JJ. Global trends in the incidence of hospital admissions for diabetes-related foot disease and amputations: a review of national rates in the 21st century. *Diabetologia*. 2023;66:267-287.
24. Chen Y, Xu Y, Cai J, et al. Automated and enclosed three-dimensional biofabrication system for mesenchymal stem cell culture to enhance diabetic wound healing. *Biomater Res*. 2025;29:0205.
25. Cacciamali A, Villa R, Dotti S. 3D cell cultures: evolution of an ancient tool for new applications. *Front Physiol*. 2022;13:836480.

26. Kusuma GD, Li A, Zhu D, et al. Effect of 2D and 3D culture microenvironments on mesenchymal stem cell-derived extracellular vesicles potencies. *Front Cell Dev Biol*. 2022;10:819726.
27. Wang G, Xie L, Li B, et al. A nanounit strategy reverses immune suppression of exosomal PD-L1 and is associated with enhanced ferroptosis. *Nat Commun*. 2021;12:5733.
28. Hu R, Lin S, Li F, et al. Exploring aptamer-based metasurfaces for label-free plasmonic biosensing of breast tumor-derived exosomes. *Adv Opt Mater*. 2024;12:2401180.
29. Navarro G, Gómez-Autet M, Morales P, et al. Homodimerization of CB(2) cannabinoid receptor triggered by a bivalent ligand enhances cellular signaling. *Pharmacol Res*. 2024;208:107363.
30. Yang Y, Zhang C, Jiang Y, et al. Harnessing cytokine-induced killer cells to accelerate diabetic wound healing: an approach to regulating post-traumatic inflammation. *Regen Biomater*. 2024;11:rbad116.
31. Huang S, Tam MY, Ho WHC, et al. Establishing a rabbit model with massive supraspinatus tendon defect for investigating scaffold-assisted tendon repair. *Biol Proced Online*. 2024;26:31.
32. Welsh JA, Goberdhan DC, O'Driscoll L, Théry C, Witwer KW. MISEV2023: an updated guide to EV research and applications. *J Extracell Vesicles*. 2024;13:e12416.
33. Busatto S, Vilanilam G, Ticer T, et al. Tangential flow filtration for highly efficient concentration of extracellular vesicles from large volumes of fluid. *Cells*. 2018;7:273.
34. Teng L, Maqsood M, Zhu M, et al. Exosomes derived from human umbilical cord mesenchymal stem cells accelerate diabetic wound healing via promoting M2 macrophage polarization, angiogenesis, and collagen deposition. *Int J Mol Sci*. 2022;23:10421.
35. Tao SC, Guo SC, Li M, Ke QF, Guo YP, Zhang CQ. Chitosan wound dressings incorporating exosomes derived from MicroRNA-126-Overexpressing synovium mesenchymal stem cells provide sustained release of exosomes and heal Full-Thickness skin defects in a diabetic rat model. *Stem Cells Transl Med*. 2017;6:736-747.
36. Lange M, Babczyk P, Tobiasch E. Exosomes: a new hope for angiogenesis-mediated bone regeneration. *Int J Mol Sci*. 2024;25:5204.
37. Liu Y, Wang M, Yu Y, Li C, Zhang C. Advances in the study of exosomes derived from mesenchymal stem cells and cardiac cells for the treatment of myocardial infarction. *Cell Commun Signal*. 2023;21:202.
38. Hu N, Cai Z, Jiang X, et al. Hypoxia-pretreated ADSC-derived exosome-embedded hydrogels promote angiogenesis and accelerate diabetic wound healing. *Acta Biomater*. 2023;157:175-186.
39. Li G, Ko CN, Li D, et al. A small molecule HIF-1alpha stabilizer that accelerates diabetic wound healing. *Nat Commun*. 2021;12:3363.
40. Yu M, Liu W, Li J, et al. Exosomes derived from atorvastatin-pretreated MSC accelerate diabetic wound repair by enhancing angiogenesis via AKT/eNOS pathway. *Stem Cell Res Ther*. 2020;11:350.
41. Valarmathi MT, Davis JM, Yost MJ, Goodwin RL, Potts JD. A three-dimensional model of vasculogenesis. *Biomaterials*. 2009;30:1098-1112.
42. Hu Y, Tao R, Chen L, et al. Exosomes derived from pioglitazone-pretreated MSCs accelerate diabetic wound healing through enhancing angiogenesis. *J Nanobiotechnology*. 2021;19:150.
43. Yan J, Tie G, Wang S, et al. Diabetes impairs wound healing by Dnmt1-dependent dysregulation of hematopoietic stem cells differentiation towards macrophages. *Nat Commun*. 2018;9:33.
44. Feng J, Dong C, Long Y, et al. Elevated kallikrein-binding protein in diabetes impairs wound healing through inducing macrophage M1 polarization. *Cell Commun Signal*. 2019;17:60.
45. He R, Yin H, Yuan B, et al. IL-33 improves wound healing through enhanced M2 macrophage polarization in diabetic mice. *Mol Immunol*. 2017;90:42-49.
46. Aitcheson SM, Frentiu FD, Hurn SE, Edwards K, Murray RZ. Skin wound healing: Normal macrophage function and macrophage dysfunction in diabetic wounds. *Molecules*. 2021;26:4917.
47. Krzyszczyk P, Schloss R, Palmer A, Berthiaume F. The role of macrophages in acute and chronic wound healing and interventions to promote pro-wound healing phenotypes. *Front Physiol*. 2018;9:419.
48. Liu YC, Zou XB, Chai YF, Yao YM. Macrophage polarization in inflammatory diseases. *Int J Biol Sci*. 2014;10:520-529.
49. Liu F, Qiu H, Xue M, et al. MSC-secreted TGF-β regulates lipopolysaccharide-stimulated macrophage M2-like polarization via the akt/FoxO1 pathway. *Stem Cell Res Ther*. 2019;10:345.
50. Tieu A, Stewart DJ, Chwastek D, Lansdell C, Burger D, Lalu MM. Biodistribution of mesenchymal stromal cell-derived extracellular vesicles administered during acute lung injury. *Stem Cell Res Ther*. 2023;14:250.
51. Lo Sicco C, Reverberi D, Balbi C, et al. Mesenchymal stem Cell-Derived extracellular vesicles as mediators of anti-inflammatory effects: Endorsement of macrophage polarization. *Stem Cells Transl Med*. 2017;6:1018-1028.
52. Liu W, Yu M, Xie D, et al. Melatonin-stimulated MSC-derived exosomes improve diabetic wound healing through regulating macrophage M1 and M2 polarization by targeting the PTEN/AKT pathway. *Stem Cell Res Ther*. 2020;11:259.
53. Watson DC, Yung BC, Bergamaschi C, et al. Scalable, cGMP-compatible purification of extracellular vesicles carrying bioactive human heterodimeric IL-15/lactadherin complexes. *J Extracell Vesicles*. 2018;7:1442088.
54. Farabi B, Roster K, Hirani R, Tepper K, Atak MF, Safai B. The efficacy of stem cells in wound healing: a systematic review. *Int J Mol Sci*. 2024;25:3006.
55. Rayat Pisheh H, Sani M. Mesenchymal stem cells derived exosomes: a new era in cardiac regeneration. *Stem Cell Res Ther*. 2025;16:16.
56. Zhu Y, Wang Y, Zhao B, et al. Comparison of exosomes secreted by induced pluripotent stem cell-derived mesenchymal stem cells and synovial membrane-derived mesenchymal stem cells for the treatment of osteoarthritis. *Stem Cell Res Ther*. 2017;8:64.